Original Research Article

Removal of Ciprofloxacin from of pharmaceutical wastewater by adsorption on SiO_2 nanoparticle

ABSTRACT

The removal of Ciprofloxacin (CFX) on SiO_2 nanoparticle was performed as a function of initial CFX concentration, contact time at fixed pH and adsorbent dose and characterized using scanning electron microscopy (SEM) and Brunauer Emmett Teller (BET) surface area. Amount of CFX uptake increased with increasing contact time and decreased concentration of initial CFX. Adsorption behavior was well described by pseudo second-order kinetic model. It was observed that equilibrium dye uptake significantly increased from 49.01 to 174.58 mg/g when initial CFX concentration increased from 25 to 100 mg/L. Experimental data were well fitted to Langmuir, Freundlich and Temkin and Dubinin-Radushkevich (D–R) models. Three different error functions were conducted to find better model to describe the experimental data. The lower values of error functions exhibited that Langmuir model was more suitable for the adsorption of CFX, which implied a homogeneous sorption phenomenon.

Keywords: SiO_2 nanoparticle; Ciprofloxacin; Error Analysis; Isotherm.

1. INTRODUCTION

Recently, pharmaceuticals have been considered as a class of emerging pollutants due to their frequent use and persistence in the environment, even at low concentration (1, 2). The introduction of these compounds in the ecosystem through anthropogenic sources can constitute a potential risk for many organisms that are present in the environment (3, 4). Other weighty contamination ways are waste effluents from hospitals and pharmaceutical industries, but there are also sewage networks and landfills (5). In fact, unused and expired drugs are usually directly discharged in the sewer network and garbage (6).

As one species of fluoroquinolone, ciprofloxacin (CIP) is frequently used and detected in the environment due to its broad-spectrum antibacterial property and high mobility (7). Furthermore, it may pose a serious risk to the living organisms by enhancing bacterial drug resistance. However, the removal of CIP from aqueous solution is difficult by present water treatment methods (8, 9).

It follows that antibiotics need to be removed before the effluents are discharged into rivers (10, 11). However, this has always been a major problem because of the difficulty of treating such wastewaters by conventional methods (12, 13). Biological procedures, although widely utilized in the removal of antibiotics, are very inefficient, because of the low biodegradability of antibiotics (14). A variety of other methods, including chemical oxidation, photocatalysis, coagulation, and electrochemical and adsorption techniques, has been examined (15, 16).

Adsorption techniques have been widely applied to the treatment of industrial wastewater containing dyes, heavy metals, and other inorganic and organic impurities (17). The adsorption phenomenon has been known since the 17th century when it was discovered that porous materials have the property of adsorbing gases and, subsequently, the same phenomenon was observed for solutions (18). Adsorption has been found to be one of the most efficient physicochemical processes, superior to many other techniques for water reuse

in terms of the simplicity of operation (19). If the adsorption system is designed correctly, it will produce a treated effluent of high quality. Activated carbon has been widely used for this purpose because of its high adsorption capacity (20). However, its high cost sometimes tends to limit its use. Several nonconventional, low-cost adsorbents have also been tried for inorganic and organic impurities removal (21, 22).
The nanotechnology and use of the nano-material is one of the effective innovations to remove the pollutants which have gained many interesting among the societies (23). The nanoparticles have been used in various studies to remove a number of pollutants such as dyes, antibiotics, heavy metals, etc (24). Those studies showed that the nanoparticles has considerable efficacy in removal of mentioned pollutants. This substantial efficacy is due to the unique features of these materials including high adsorption capacity, simplicity in operation, rapid adsorption process, etc (25).

Objective of the present study, were to examine the potential of a SiO_2 nanoparticle for the removal of commonly used antibiotics, CFX and to determine equilibrium and kinetic parameters for CFX in a batch system as a function of initial CFX concentration and contact time.

2. MATERIALS AND METHODS

Ciprofloxacin was obtained from Sigma (Sigma–Aldrich Chemical Co., St. Louis, USA). The chemical structure and properties of CFX is given in Table 1. Stock CFX solution was prepared in distilled water as 1.0 g/L. For the adsorption studies, the adsorbent suspension was prepared by using this SiO_2 nanoparticle. Adsorption studies were performed in 250 mL Erlenmeyer flask containing 100 mL of CFX solution at different concentrations. The pH of each solution was adjusted to required value with diluted or concentrated HCl and NaOH solutions before mixing the adsorbate and adsorbent. The initial CFX concentrations were adjusted to 25, 50, 75 and 100 mg/L. These flasks were agitated on the orbital shaker at 150 rpm for 90 min to ensure equilibrium. Samples (10 mL) were taken before mixing of adsorbent suspension with CFX bearing solution, then at time intervals (10, 20, 30, 45, 60, 75, 90 and 120 min) for the determination of residual CFX concentration. After that, samples were centrifuged to precipitate suspended biomass at 3600 rpm for 10 min. The concentration of CIP in the solution after equilibrium was determined by a HPLC (C18 ODS column) with a UV detector 2006 at a wavelength of 277 nm. The mobile phase was 0.05 M phosphoric acid/acetonitrile with a volumetric ratio of 87/13 with an injection flow rate of 1 mL/min. Duplicates experiments were carried out and used data in the present study were the mean values of two replicate determinations. Amount of CFX uptake per unit mass of adsorbent at time t (q_t, mg/g) and at equilibrium (q_e, mg/g) were calculated by using Eqs. (1) and (2), respectively (26, 27):

$$q_t = \frac{(C_0 - C_t)V}{M}$$

$$q = \frac{(C_0 - C_e)V}{M}$$

Where C_0, Ct and C_e represent at initial, at t time and at equilibrium concentrations of CFX (mg/L) in the solution, respectively. V is the volume of solution (L), and M is the mass of adsorbent (g).

Table 1. Ciprofloxacin molecular structure and physical chemical properties

Parameter	Character/ Value
Molecular structure	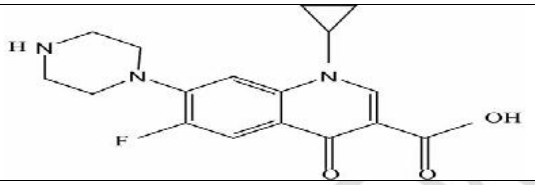
CAS number	85721-33-1
Molecular formula	$C_{17}H_{18}FN_3O_3$
Molecular weight	331.35 g/mol
Solubility in water	150–6190 mg/L at 20°C

3. RESULTS AND DISCUSSION

The CFX nanoparticles were purchased from Research Institute of Petroleum Industry (RIPI), Tehran, Iran which was used to study the adsorption characteristics of CFX from aqueous solutions. The outer diameter of SiO_2 nanoparticles used in this study was in range of 10 to 20 nm. In addition, the specific surface area of SiO_2 nanoparticles was reported to be greater than 210 m^2/g and the mass ratio of the amorphous carbon of SiO_2 nanoparticles was lesser than 10%. The SEM images of this adsorbent were provided, using a Philips XL30 scanning electron microscope (SEM). This image (Fig. 1) shows the porous surface of this adsorbent and reveals that it can be proper adsorbent for CFX removal.

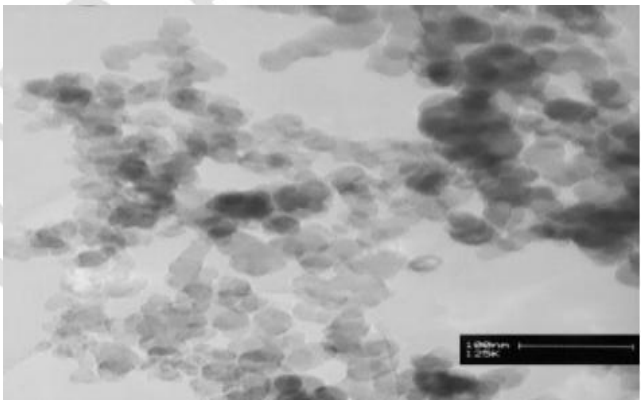

Fig. 1. The SEM image of the SiO2 nanoparticle

3.1. Adsorption isotherms

Adsorption isotherm studies using linear form models. The adsorption data that depends on the extent of adsorption with the increase in CFX concentration were analyzed using isotherm models; Freundlich, Langmuir, Temkin, and Dubinin–Radushkevich (D–R) models in linear form and its corresponding isotherm parameters were evaluated.

Langmuir isotherm model demonstrates a monolayer adsorption mechanism with homogeneous adsorption energies and is described by the following Eq. (3) (28, 29):

$$\frac{1}{q_e} = \frac{1}{q_m} + \frac{1}{q_m K_L} \times \frac{1}{C_e}$$

Where q_m and K are Langmuir constants related to monolayer adsorption capacity (mg/g) and adsorption energy (L/mg), respectively.

Freundlich isotherm model describes the multilayer adsorption of lead ions on the adsorbent surface with heterogeneous surface energy and is expressed in the linear form as Eq. (4) (30, 31):

$$\mathrm{Log} q_e = \log K_F + \frac{1}{n} \mathrm{Log} C_e$$

Where q_e (mg/g) is the amount of CFX adsorbed per gram of adsorbent at equilibrium, Ce (mg/L) is the equilibrium concentration of CFX remained in the solution, K_F and 1/n are Freundlich constants that can be related to the adsorption capacity of the adsorbent ((mg/g)(L/mg)$^{1/n}$) and the intensity of adsorption, respectively.

Temkin isotherm model assumes that the heat of adsorption of ions in the layer decreases linearly with coverage, which is due to the adsorbate and adsorbate interactions. Temkin model is given by Eq. (5) (32, 33):

$$q_e = \mathrm{B} \ln \mathrm{K_T} + B \ln \mathrm{C_e} \quad \mathrm{B} = \frac{\mathrm{RT}}{\mathrm{b}}$$

Where b is the Temkin constant (J/mol) related to the adsorption heat, T is the absolute temperature (K), R is the gas constant (8.314 J/mol K), and K_T is the Temkin isotherm constant (L/g).

Dubinin-Radushkevich (D–R) isotherm model is applied to identify the nature of adsorption processes. The linear form of D–R isotherm equation is given by Eq. (6) (34, 35):

$$\log q_e = \ln \mathrm{q_m} - \beta \varepsilon^2$$

Where q_e is the adsorption capacity (mol/g), q_m is the maximum adsorption capacity, i.e. the amount of CFX at complete monolayer coverage (mol/g), β is the parameter related to the adsorption energy (mol^2/kJ^2) and ε is the Polanyi potential (ε = RT Ln (1 + 1/C_e). The value of K_D is related to the adsorption energy, E (kJ/mol), which is defined as the free energy change required to transfer a molecule from solution to the solid surfaces. The adsorption energy can be calculated by Eq. (7) (36, 37):

$$\mathrm{E} = \frac{1}{\sqrt{2\beta}}$$

A plot of Ln q_e vs. ε^2 will give the values of β and q_m from the slope and intercept.

The adsorption energy, E, gives information about adsorption mechanism as chemical ion-exchange or physical adsorption. If E value <8 kJ/mol, the adsorption is physical in nature, whereas, if 8<E<16 kJ/mol, the ion exchange is the adsorption mechanism, while if E>16 kJ/mol, the chemical adsorption occur.

The dimensionless separation factor (R_L), defined by Eq. (8), is an important characteristic of Langmuir isotherm. This factor explains the nature of the adsorption process on the adsorbent (R_L>1, unfavorable; R_L=1, linear; 0<R_L<1, favorable; and R_L>0, irreversible (38, 39):

$$\mathrm{R_L} = \frac{1}{1 + \mathrm{K_L C_0}} \qquad (8)$$

The values of isotherm constants and the correlation coefficients (R^2) are presented in Table 2. The standard deviation (SD) and the statistical errors as the residual sum of square error (RSSE) and the root mean square error (RMSE) are also placed in Table 1 and calculated according to Eqs. (9)-- (11) as follow (40-42):

$$SD= \sqrt{\frac{\sum[(q_{e\ exp}-q_{e\ cal})/qe\ cal]^2}{N-1}} \times 100 \qquad (9)$$

$$RSSE= \sum_{I=1}^{N_e}(q_{\ exp} - q_{e\ cal})^2 \qquad (10)$$

$$RMSE= \sqrt{\sum_{I=1}^{N_e}[\frac{(q_{e\ exp}-q_{e\ cal})^2}{N_e}]} \qquad (11)$$

Where $q_{e\ exp}$ and $q_{t\ cal}$ are the amounts of CFX adsorbed experimentally and calculated from the model at time t, respectively, N is the number of experimental data points, and e is the number of parameters in the model. A model is considered as good if the correlation coefficient (R^2) is high, and all statistical errors and SD are minimum. From Table 2, it was observed that the Langmuir isotherm model has higher correlation coefficient (R^2) and lower in SD, RMSE, and RSSE when compared to the other models.

Where R^2 for adsorption of CFX onto SiO_2 nanoparticle are 0.999, 0.794, 0.803, and 0.946 for Langmuir, Freundlich, Temkin, and D–R isotherm models, respectively. Also, SD, RMSE and RSSE of Langmuir model are 0.0071, 0.146, and 0.595, which are lower than that for the other models. Thus the isotherm data follow the Langmuir model. Therefore, the adsorption process of CFX onto SiO_2 follows the Langmuir isotherm model, indicating a monolayer adsorption sites with homogeneous nature of the adsorbent without any interaction between adsorbed molecules. R_L values were calculated from the entire concentration range studied and presented in Table 1. From this table, it shows that the value of separation factor (R_L) is 0.0632, indicating favorable adsorption. The calculated E values for CFX adsorption onto SiO_2 nanoparticle was 2.241 kJ/mol, thereby suggesting that the adsorption process may be carried out via physical adsorption.

Table 2: Isotherm constants for the adsorption of CFX onto SiO_2 nanoparticle

Langmuir		D-R		Freundlich		Temkin	
q_m	174.5	q_m	115.6	K_F	5.415	K_T	0.372
R_L	0.0632	E	2.241	n	1.652	B	5.192
R^2	0.9991	R^2	0.946	R^2	0.794	R^2	0.803
SD	0.0071	SD	1.754	SD	3.495	SD	3.461
RMSE	0.146	RMSE	4.684	RMSE	6.518	RMSE	8.172
RSSE	0.0595	RSSE	3.125	RSSE	8.721	RSSE	5.925

3.2. Adsorption kinetics

The effects of contact time on the adsorption of CFX onto SiO_2 and the percentage of CFX removed at four different initial CFX concentrations are illustrated in Fig. 2. Hence it appears that a rapid initial uptake occurs, with equilibrium reached in less than 30 min. The adsorption capacity at equilibrium increased from 49.01 to 174.58 mg/g, as the initial CFX concentration increased from 25 to 100 mg/L. Particularly noteworthy is the speed of adsorption for all concentrations, a feature common to all the other initial CFX concentrations studied in this work irrespective of the temperature. Thus, a contact time of less than 30 min

was invariably sufficient to reach equilibrium. The fast uptake of the CFX molecules is due to solute transfer, as there are only sorbate and sorbent interactions with negligible interference from solute solute interactions.

The adsorption kinetics of CFX onto SiO_2 nanoparticle is already apparent in Fig. 2 at the initial concentrations of 25, 50, 75 and 100 mg/L. The data were analyzed by applying pseudo-first-order (Eq. 12), pseudo-second-order (Eq. 13), and intraparticle diffusion (Eq. 14) models in order to gain a better understanding of the adsorption process (43-46).

$$\text{Log}\,(q_e - q_t) = \log q_e - \frac{K_1}{2.303}t \qquad (12)$$

$$\frac{t}{q_t} = \frac{1}{k_2 qe^2} + \frac{t}{qe} \qquad (13)$$

$$q_t = K_d\, t^{0.5} + I \qquad (14)$$

In the above equations, q_e (mg/L) and q_t (mg/L) are the amounts of CFX adsorbed at equilibrium and at any contact time of adsorption t (min), respectively; K_1 (1/h), K_2 (g/mg. h), and K (mg/g. $h^{1/2}$) are the pseudo-first-order, pseudo-second-order, and intraparticle diffusion rate constants, respectively. According to Eq. (12), the plot of Ln ($q_e - q_t$) versus t, and according to Eq. (14), the plot of q_t versus $t^{1/2}$ should each give a straight line for the respective model to be applicable. However, neither equation fitted well for the whole range of concentrations at any contact time, showing poor correlation coefficient values. Accordingly, the experimental data do not conform to either of these models. According to Eq. (13), the plot of t/q_t against t should be linear, as is shown in fact to be the case (Fig. 3). The pseudo-second-order rate constant K_2 and the corresponding linear regression correlation coefficient values, R^2 and, are given in Table 2. From Table 2, it was observed that the Langmuir isotherm model has higher correlation coefficient (R^2=0.997–0.999) and lower in SD, RMSE, and RSSE when compared to the other models at all concentrations. These results indicate that the adsorption data conform well to pseudo-second-order kinetics for the entire adsorption process.

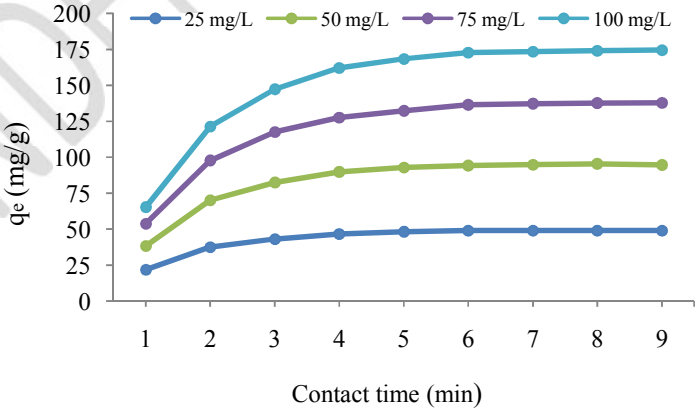

Fig. 2. Effect of contact time on the adsorption of MB onto MC (adsorbent dose = 0.5 g/L, pH = 7, temp = 30 ± 2 °C)

Table 3: the results of kinetic model studies related to the CFX adsorption onto SiO_2 nanoparticle

C0 (mg/L)	$(q_e)_{exp}$	Intraparticle diffusion					
		K_d	I	R^2	SD	RMSE	RSSE
25	9.981	0.819	11.82	0.841	1.414	3.512	5.612
50	24.82	0.711	14.71	0.795	2.198	5.498	3.745
75	47.09	0.521	19.24	0.824	1.728	6.147	4.159
100	84.72	0.307	21.46	0.819	2.746	3.866	4.045
C_0 (mg/L)	$(q_e)_{exp}$	Pseudo-first order					
		$(q_e)_{cal}$	K_1	R^2	SD	RMSE	RSSE
25	9.981	3.127	0.059	0.789	3.156	6.197	3.115
50	24.82	8.341	0.047	0.848	3.875	5.852	3.954
75	47.09	14.36	0.038	0.871	4.189	6.963	4.154
100	84.72	29.34	0.026	0.869	5.951	7.452	4.872
C0 (mg/L)	$(q_e)_{exp}$	Pseudo-second order					
		$(q_e)_{cal}$	K_2	R^2	SD	RMSE	RSSE
25	9.981	9.064	0.068	0.998	0.084	1.086	1.295
50	24.82	22.73	0.041	0.999	0.095	0.842	1.046
75	47.09	41.35	0.015	0.997	0.484	0.691	0.829
100	84.72	81.64	0.0084	0.998	0.545	0.486	0.446

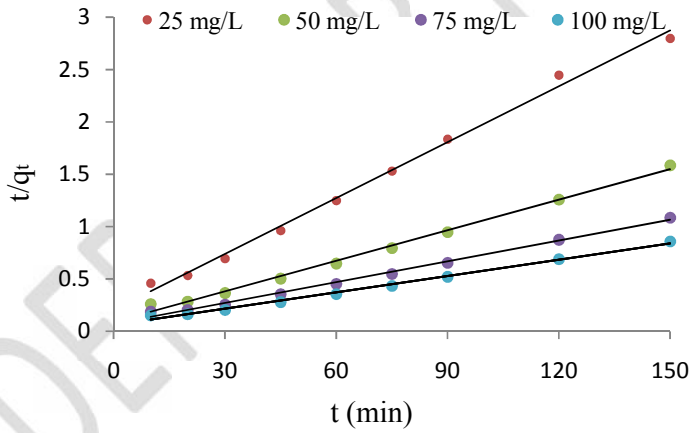

Fig. 3. Pseudo-second order Kinetic models for CFX adsorption at different concentrations

4. CONCLUSION

The present study revealed SiO_2 nanoparticle had a potential to remove CFX from aqueous solution. The behavior of batch adsorption kinetics was well described by pseudo-second-order kinetic model. From the results of R^2 and the error functions, Langmuir models were well fitted to the experimental data than those of Freundlich and Temkin, and Dubinin–Radushkevich (D–R) model.

CONSENT

It is not applicable.

ETHICAL APPROVAL

It is not applicable.

ACKNOWLEDGEMENTS

The authors would like to acknowledge from Zahedan University of medical sciences for the support this study.

COMPETING INTERESTS

Authors have declared that no competing interests exist.

REFERENCES

1. Balarak D, Mostafapour FK, Joghataei A. Experimental and Kinetic Studies on Penicillin G Adsorption by Lemna minor. British J Pharm Res. 2016; 9(5): 1-10.
2. Hu L, Flanders PM, Miller PL, Strathmann TJ. Oxidation of sulfamethoxazole and related antimicrobial agents by TiO_2 photocatalysis Water Research 2007; 41(12); 2612-26.
3. Yu F, Li Y, Han S, Jie Ma J. Adsorptive removal of antibiotics from aqueous solution using carbonMaterials. Chemosphere. 2016; 153; 365–85.
4. Balarak D, Mostafapour FK, Azarpira H. kinetic and Equilibrium Studies of Sorption of Metronidazole Using Graphene Oxide. British J Pharm Res. 2017; 19 (4); 1-10.
5. Ji L, ChenW, Duan L and Zhu D. Mechanisms for strong adsorption of tetracycline to carbon nanotubes: A comparative study using activated carbon and graphite as adsorbents. Environ Sci Technol. 2009, 43 (7), 2322–27.
6. Balarak D, Azarpira H, Mostafapour FK. Study of the Adsorption Mechanisms of Cephalexin on to Azolla Filiculoides. Der Pharma Chemica. 2016, 8(10):114-121.
7. Chena H, Bin Gaoa B, Lib H. Removal of sulfamethoxazole and ciprofloxacin from aqueous solutions by graphene oxide. Journal of Hazardous Materials.2015; 283; 201-07.
8. Balarak, D, Joghataei A, Mostafapour FK. Ciprofloxacin Antibiotics Removal from Effluent Using Heat-acid Activated Red Mud. British J Pharm Res. 2017; 20(5); 1-11.
9. Balarak D, Mostafapour FK, Joghataei A. Kinetics and mechanism of red mud in adsorption of ciprofloxacin in aqueous solution. Biosci Biotechnol Res commun. 2017; 10(1);241-248.
10. Garoma T, Umamaheshwar SH, Mumper A. Removal of sulfadiazine, sulfamethizole, sulfamethoxazole, and sulfathiazole from aqueous solution by ozonation. Chemosphere. 2010; 79; 814–20.
11. Rostamian R, Behnejad H. A comparative adsorption study of sulfamethoxazole onto graphene and graphene oxide nanosheets through equilibrium, kinetic and thermodynamic modeling. Process Safety and Environmental Protection.2016; 102; 20-29.
12. .34 Balarak D, Mostafapour FK, Azarpira H. Langmuir, Freundlich, Temkin and Dubinin-radushkevich Isotherms Studies of Equilibrium Sorption of Ampicilin unto Montmorillonite Nanoparticles. British J Pharm Res.2016; 20 (2); 1-10.
13. Zhu XD, Wang YJ, Sun RJ, Zhou DM. Photocatalytic degradation of tetracycline in aqueous solution by nanosized TiO2. Chemosphere. 2013; 92; 925–32.
14. Balarak D, Azarpira H,. Rice husk as a Biosorbent for Antibiotic Metronidazole Removal: Isotherm Studies and Model validation. International Journal of ChemTech Research. 2016; 9(7); 566-573.
15. Ji L, Chen W, Duan L and Zhu D. Mechanisms for strong adsorption of tetracycline to carbon nanotubes: A comparative study using activated carbon and graphite as adsorbents. Environ. Sci. Technol., 2009, 43 (7), 2322–27.
16. Choi KJ, Kim SG, Kim SH. Removal of antibiotics by coagulation and granular activated carbon filtration. J. Hazard. Mater. 2008; 151; 38–43.
17. 4Su YF, Wang GB, Kuo DTF, Chang ML. Photoelectrocatalytic degradation of the antibiotic sulfamethoxazole using TiO2/Tiphotoanode. Applied Catalysis B: Environmental. 2016; 186; 184-92.
18. Rostamian R, Behnejad H. A comparative adsorption study of sulfamethoxazole onto graphene and graphene oxide nanosheets through equilibrium, kinetic and thermodynamic modeling. Process Safety and Environmental Protection.2016; 102; 20-29.
19. Balarak D, Mostafapour FK, Joghataei A. Biosorption of amoxicillin from contaminated water onto palm bark biomass. Int J Life Sci Pharma Res. 2017; 7(1);9-16

20. Balarak D, Mostafapour FK. Batch Equilibrium, Kinetics and Thermodynamics Study of Sulfamethoxazole Antibiotics onto Azolla filiculoides as a Novel Biosorbent. British J Pharm Res. 2016; 13 (2); 1-10.
21. Li B, Zhang T. Biodegradation and adsorption of antibiotics in the activated sludge process. Environmental Science & Technology. 2010; 44:3468–3473.
22. Perez S, Eichhorn P, Aga DS. 2005. Evaluating the biodegradability of Sulfamethazine, sulfamethoxazole, sulfathiazole, and trimethoprim at different stages of sewage treatment. Environmental Toxicology and Chemistry 24:1361–1367.
23. Zhang L, Song X, Liu X, Yang L, Pan F, Lv J. Studies on the removal of tetracycline by multi-walled carbon nanotubes, Chem. Eng. J. 2011; 178; 26–33.
24. Balarak D, Mahdavi Y, Maleki A, Daraei H and Sadeghi S. Studies on the Removal of Amoxicillin by Single Walled Carbon Nanotubes. British J Pharm Res 2016;10(4): 1-9
25. Balarak D, Mahdavi Y and Mostafapour FK. Application of Alumina-coated Carbon Nanotubes in Removal of Tetracycline from Aqueous Solution. British J Pharm Res. 2016; 12(1): 1-11.
26. Gulkowsk A, Leung HW, So MK, Taniyasu S, Yamashita N. Removal of antibiotics from wastewater by sewage treatment facilities in Hong Kong and Shenzhen, China. Water Research. 2008; 42:395-403.
27. Aksu Z, Tunc O. Application of biosorption for Penicillin G removal: Comparison with activated carbon. Process Biochemistry. 2005;40(2):831-47.
28. Braschi I, Blasioli S, Gigli L, Gessa CE, Alberti A,Martucci A. Removal of sulfonamide antibiotics from water: evidence of adsorption into an organophilic zeolite Y by its structural modifications. Journal of Hazardous Materials. 2010; 178:218–225.
29. Gao J and Pedersen JA. Adsorption of Sulfonamide Antimicrobial Agents to Clay Minerals. Environ. Sci. Technol. 2005, 39(24). 9509-16.
30. Putra EK, Pranowoa, Sunarsob J, Indraswatia N, Ismadjia S. Performance of activated carbon and bentonite for adsorption of amoxicillin from wastewater: mechanisms, isotherms and kinetics. Water Res. 2009; 43, 2419-30.
31. Dutta M, Dutta NN, Bhattachary KG. Aqueous phase adsorption of certain beta-lactam antibiotics onto polymeric resins and activated carbon. Separation and Purification Technology.1999;16(3);213-24.
32. Balarak D, Mostafapour FK, Akbari, H. Adsorption of Amoxicillin Antibiotic from Pharmaceutical Wastewater by Activated Carbon Prepared from Azolla filiculoides. British J Pharm Res. 2017; 18(3); 1-10.
33. Balarak D, Azarpira H. Photocatalytic degradation of sulfamethoxazole in water: investigation of the effect of operational parameters. Inter J Chem Tech Res. 2016; 9(12):731-8.
34. Balarak D, Mostafapour FK, Azarpira H. Adsorption Kinetics and Equilibrium of Ciprofloxacin from Aqueous Solutions Using Corylusavellana (Hazelnut) Activated Carbon. British J Pharm Res.2016; 13 (3); 1-10.
35. Rivera-Jiménez SM, Hernández-MaldonadoAJ. Nickel(II) grafted MCM-41: A novel sorbent for the removal of Naproxen from water. Microporous and Mesoporous Materials. 2008;116(1-3); 246–52.
36. Adrianoa WS, Veredasb V, Santanab CC, Gonçalves LRB. Adsorption of amoxicillin on chitosan beads: Kinetics, equilibrium and validation of finite bath models. Biochemical Engineering Journal. 2005; 27(2) ;132-37.
37. Erşan M, Bağd E. Investigation of kinetic and thermodynamic characteristics of removal of tetracycline with sponge like, tannin based cryogels. Colloids and Surfaces B: Biointerfaces. 2013; 104;75-82.
38. HuangM, Tian S, Chen D, ZhangW,Wu J, Chen L. Removal of Sulfamethazine antibiotics by aerobic sludge and an isolated Achromobacter sp S-3. Journal of Environmental Sciences-China. 2012; 24:1594–159.
39. Peterson JW. Petrasky LJ, Seymourc MD, Burkharta RS, Schuiling AB. Adsorption and breakdown of penicillin antibiotic in the presence of titanium oxide nanoparticles in water. Chemosphere. 2012;87(8); 911-7.

40. Chen WR, Huang CH. Adsorption and transformation of tetracycline antibiotics with aluminum oxide. Chemosphere. 2010; 79, 779-85.
41. Balarak D, Mostafapour FK, Bazrafshan E, Saleh TA. Studies on the adsorption of amoxicillin on multi-wall carbon nanotubes. Water Sci technol. 2017; 75(7); 1599-1606 .
42. Balarak D, Mostafapour FK. Batch Equilibrium, Kinetics and Thermodynamics Study of Sulfamethoxazole Antibiotics Onto Azolla filiculoides as a Novel Biosorbent. British J Pharm Res.2017;13(2); 1-11 .
43. Balarak D, Mostafapour FK, Khatibi AD. Nonlinear Isotherms and Kinetics and Application Error Functions for Adsorption of Tetracycline on Lemna Minor. British J Pharm Res. 2018;23(2); 1-11 .
44. Yu F, Li Y, Han S, Jie Ma J. Adsorptive removal of antibiotics from aqueous solution using carbon Materials. Chemosphere. 2016;153;365–385.
45. Balarak D, Mostafapour FK, Joghataei A. Thermodynamic Analysis for Adsorption of Amoxicillin onto Magnetic Carbon Nanotubes. British J Pharm Res.2017; 16 (6); 1-10.
46. Mostafapour FK ; Dashtizade M; Balarak D. Adsorption Thermodynamics, Kinetics and Mechanism for the Adsorption of Erythromycin onto Multi-Walled Carbon Nanotubes. British J Pharm Res. 2018;24(6); 1-11.